Advances in Nano Research, *Vol. 13, No.4 (2022) 393-406*
https://doi.org/10.12989/anr.2022.13.4.393

Nonlinear bending and post-buckling behaviors of FG small-scaled plates based on modified strain gradient theory using Ritz technique

S. Amir M. Ghannadpour* and Selma Khajeh

Faculty of New Technologies Engineering, Shahid Beheshti University, Tehran, Iran

(*Received October 14, 2021, Revised April 5, 2022, Accepted April 12, 2022*)

Abstract. In the present article, functionally graded small-scaled plates based on modified strain gradient theory (MSGT) are studied for analyzing the nonlinear bending and post-buckling responses. Von-Karman's assumptions are applied to incorporate geometric nonlinearity and the first-order shear deformation theory is used to model the plates. Modified strain gradient theory includes three length scale parameters and is reduced to the modified couple stress theory (MCST) and the classical theory (CT) if two or all three length scale parameters become zero, respectively. The Ritz method with Legendre polynomials are used to approximate the unknown displacement fields. The solution is found by the minimization of the total potential energy and the well-known Newton-Raphson technique is used to solve the nonlinear system of equations. In addition, numerical results for the functionally graded small-scaled plates are obtained and the effects of different boundary conditions, material gradient index, thickness to length scale parameter and length to thickness ratio of the plates on nonlinear bending and post-buckling responses are investigated and discussed.

Keywords: FG small-scaled plates; length scale; modified couple stress theory; modified strain gradient theory; nonlinear bending; post-buckling behavior

1. Introduction

Functionally graded materials (FGMs) have received remarkable attention for different industrial applications because of ultrahigh temperature resistant properties. FGMs are inhomogeneous materials in which material properties change gradually and continuously in some directions. They are mixed of different materials and are usually made of metal and ceramic. These materials were introduced for the first time by Koizumi (1997) and studied in many works. For example, Alinia and Ghannadpour (2009) studied nonlinear bending analysis of square plates made of functionally graded materials. Ghannadpour *et al*. (2012) investigated the buckling behavior of rectangular functionally graded plates (FGPs) and post-buckling behavior of FGPs in thermal environments was studied by Ovesy *et al*. (2015). Nowadays, increasing attention is being paid to the use of beams and plates on small scale and in micro-electro-mechanical systems (MEMSs) and nano-electro-mechanical systems (NEMSs) (Hassanpour *et al*. 2007, Sheng *et al*. 2010). Some studies have shown that the size of the structure affects its behavior at the nano- and micro-scales and cannot be ignored (Nix 1989, Fleck *et al*. 1994, Fenjan *et al*. 2020, Fantuzzi *et al*. 2021, Avey *et al*. 2021, Mahmure, *et al*. 2021). However, the classical theories of elasticity cannot predict size effects due to the lack of additional material length scale parameters. Therefore, higher-order continuum theories, such as couple stress theories (Toupin 1962), strain gradient theories (Zibaei *et al*. 2014, Jena *et al*. 2019), nonlocal elasticity theories (Taghizadeh *et al*. 2015, Mehar *et al*. 2018), micro-morphic (Tavakolian *et al*. 2017) and micro-polar (Eringen 1966, 1967, Tuna and Trovalusci 2020) are used which include additional small-scale parameters and play an indicator role in considering the mechanical behavior of micro-structures. Ghannadpour and Moradi (2019) and Ghannadpour *et al*. (2020) investigated the effects of small-scale parameters in their research to study the nonlocal nonlinear analysis and post-buckling behavior of nano-graphene sheets. One of the theories of higher-order elasticity was known as the couple stress theory (CST) introduced by Mindlin and Tiersten (1962) and Koiter (1969) that uses two classical material constants and two material length scale parameters to survey the small-scale effects. Different versions of couple stress theory examined by Hadjesfandiari and Dargush (2016) and it was developed by Shariati *et al*. (2020) to apparent the frequency retaliation of FG nano-beams. The strain gradient theory (SGT) was presented by Mindlin (1965) where the first and second derivatives of the strain tensor influencing the strain energy density are considered. Bensaid *et al*. (2018) employed the nonlocal strain gradient theory to investigate free vibrations of nano-beams resting on elastic foundations. The modified strain gradient theory (MSGT) was studied by Yang *et al*. (2002) in which constitutive relationships caused a reduction in number of length-scale parameters from two in the CST to one. Moreover, the modified strain gradient theory (MSGT) was developed by Lame *et al*. (2003). MSGT reduces the five scale constants in strain gradient theory to three. The names of these constants are dilatation gradient, deviatoric gradient and symmetric rotation gradient tensors. Due to the importance and wide application of FG micro-plates, the analysis of

*Corresponding author, Associate Professor,
E-mail: a_ghannadpour@sbu.ac.ir

ISSN: 2287-237X (Print), 2287-2388 (Online)

these plates by these theories has received much attention from researchers. Tsiaste (2009) developed the governing equations of the Kirchhoff plate with the most common type of boundary conditions based on modified couple stress theory. The size-dependent vibration analysis of Kirchhoff plate was derived by Jomezadeh *et al*. (2011). In addition, Asghari *et al*. (2011) investigated the static bending and free vibration of cantilever and simply-supported for Timoshenko beams made of functionally graded materials (FGM) based on MCST. The modified couple stress theory and Mindlin plate theory were applied to analyze bending, buckling, and vibration of annular micro-plates made of functionally graded materials (FGMs) by Ke *et al*. (2012). Also, in another work, axisymmetric post-buckling of FG annular micro-plates was studied by Ke *et al*. (2014) by taking the position of the physical neutral plane into account, which can help with the removal of stretching-bending coupling effects. Thai and Choi (2013) presented the bending, buckling, and free vibration of functionally graded Kirchhoff and Mindlin plates by applying the modified couple stress theory and Hamilton's principle for simply-supported boundary conditions. Ansari *et al*. (2015) examined the nonlinear bending behavior of FG micro-plates considering the neutral plane according to the MCST. In this study, the governing equations and boundary conditions were solved by using the GDQ method and pseudo-arclength continuation. Moreover, based on MCST with damping effect, Akbas (2018) analyzed forced vibrations in a cracked functionally graded micro-beam. Papargyri-Beskou and Beskos (2008) analyzed gradient elastic flexural plates using a Kirchhoff micro-plate and carried out results from statics, stability, and dynamic analyses.

The size effect on the bending of thin strain gradient elastic plates was studied by Lazopoulos (2009) using the Kirchhoff plate theory. A gradient elastic flexural Kirchhoff plate under static load was computed by Papargyri-Beskou *et al*. (2010) using a variational method. Based on strain gradient elasticity theory, Wang *et al*. (2010) have developed a micro-scale Timoshenko beam model to study the size effect and also a finite element method was employed by Bacciocchi *et al*. (2021) to estimate critical buckling loads and natural frequencies of laminated Kirchhoff plates, taking into account the nonlocal strain gradient effect. By using the second-order strain gradient theory developed by Monaco *et al* (2021), vibrations and buckling of thin laminated nano-plates in hygrothermal environment have been investigated. In this research, Hamilton's principle has been used to obtain equations of motion. They also investigated the bending behavior of magneto-electro-elastic strain gradient nonlocal nano-plates in hygrothermal environment, using a trigono-metric approach. In another study, they obtained critical temperatures for vibrations and buckling of nano-plates. The nano-plates had a coupled magneto-electro-elastic constitutive equation in a hygrothermal environment. Furthermore, Akgöz and Civalek (2013) used Bernoulli-Euler beams and modified strain gradient theory to model the buckling behavior of functionally graded micro-beams for various boundary conditions. Mohammadi *et al*. (2010) also studied a size dependent Kirchhoff plate for determining

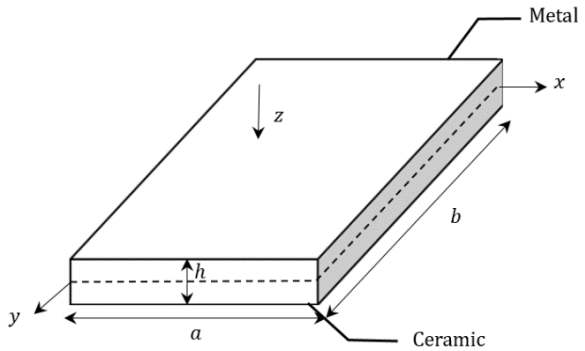

Fig. 1 A typical FG micro-plate

the buckling loads of rectangular micro-plates based on the MSGT and MCST by using the variational approach and principle of minimum total potential energy. Also, a Kirchhoff micro-plate based on modified strain gradient elasticity theories and modified couple stress theories was studied by Movassagh and Mahmoodi (2013). These studies apply the extended Kantorovich method (EKM) in order to solve the boundary value problems of sixth order. Next, Ansari *et al*. (2016) employed size dependent of first-order shear deformation plate theory (FSDT) to describe nonlinear bending analysis based on the MSGT and MCST using quadrilateral finite element method. Meanwhile, a free vibrational analysis of three-dimensional functionally graded nano-plates with small-scale effects has been carried out by Dehshari *et al*. (2020) using MSGT.

This research studies nonlinear bending and post-buckling of size dependent micro-plates based on the MSGT, MCST and classical theory of elasticity. Three length-scale parameters are required in the MSGT formulation, which can be reduced to a single parameter in the MCST formulation. The formulation is also written based on the FSDT and Von-Karman's assumptions. Therefore, to approximate the unknown displacement fields, Ritz technique and Legendre polynomials are developed. Nonlinear equilibrium equations are derived by applying the minimum total potential energy principle and solved using the Newton-Raphson method. The effects of thickness to length scale parameter, material gradient index, length to thickness ratio of the micro-plates and boundary conditions of the FG micro-plates are surveyed.

2. Theoretical formulation

FG micro-plates in this research with dimensions a, b and h are assumed to be composed of two materials, ceramic and metal, with the ceramic at the bottom surface (i.e., at $z = h/2$) and metal at the top surface.

The material properties of FG micro-plates including Young modulus $E(z)$ and Poisson's ratio $\nu(z)$ can be estimated by the simple power law as follow:

$$E(z) = E_m + (E_c - E_m)\left(\frac{1}{2} + \frac{z}{h}\right)^k$$
$$\nu(z) = \nu_m + (\nu_c - \nu_m)\left(\frac{1}{2} + \frac{z}{h}\right)^k \quad (1)$$

where the subscripts c and m represent ceramic and metal, respectively and k indicates the material gradient index. It is known that the FG plate with $k = 0$ is fully ceramic and with $k \to \infty$ is fully metal. The physical neutral plane is not equal to the geometric middle plane for inhomogeneous functionally graded micro-plates, thus, by choosing the physical neutral plane as the reference plane, the stretching-bending coupling stiffness can be ignored.

$$\bar{z} = z - z_0$$

$$z_0 = \frac{\int_{-h/2}^{h/2} (\lambda + 2\mu) z \, dz}{\int_{-h/2}^{h/2} (\lambda + 2\mu) \, dz} \tag{2}$$

In which z_0 represents the z-coordinate of the physical neutral plane and $\lambda = \frac{E(z)\nu(z)}{1-\nu(z)^2}$ and $\mu = \frac{E(z)}{2(1+\nu(z))}$ are the bulk and shear modules, respectively.

According to the first-order shear deformation plate theory, the displacements at a general point in the plate can be computed by the following equations in which u, v and w are in-plane and out-of-plane displacements of mid-plane and φ_x and φ_y represent the rotations of a transverse normal about y- and x-axes, respectively.

$$\begin{aligned} u_x(x,y,z) &= u(x,y) + \bar{z}\varphi_x(x,y) \\ u_y(x,y,z) &= v(x,y) + \bar{z}\varphi_y(x,y) \\ u_z(x,y,z) &= w(x,y) \end{aligned} \tag{3}$$

Based on modified strain gradient theory, the total energy density of deformation depends on four factors; the symmetric strain tensor, the dilatation gradient tensor, the deviatoric stretch gradient tensor, and the symmetric rotation gradient tensor. The strain energy (Π_S) of a deformed linear elastic material is given by:

$$\Pi_S = \frac{1}{2}\int_\Omega \left(\sigma_{ij}\varepsilon_{ij} + p_i\gamma_i + \tau_{ijk}^{(1)}\eta_{ijk}^{(1)} + m_{ij}^s\chi_{ij}^s\right) d\Omega \tag{4}$$

where $\varepsilon_{ij}, \gamma_i, \eta_{ijk}^{(1)}, \chi_{ij}^s (i,j,k = x,y,z)$ represent the components of the strain tensor, the dilatation gradient tensor, the deviatoric stretch gradient tensor and the symmetric rotation gradient tensor, respectively, expressed as below by Lame *et al*. (2003):

$$\varepsilon_{ij} = \frac{1}{2}\left(u_{i,j} + u_{j,i} + u_{k,i}u_{k,j}\right) \tag{5}$$

$$\gamma_i = \varepsilon_{mm,i} \tag{6}$$

$$\eta_{ijk}^{(1)} = \eta_{ijk}^s - \frac{1}{3}\left(\delta_{ij}\eta_{mmk}^s + \delta_{jk}\eta_{mmi}^s + \delta_{ki}\eta_{mmj}^s\right) \tag{7}$$

$$\eta_{ijk}^s = \frac{1}{3}\left(\varepsilon_{jk,i} + \varepsilon_{ki,j} + \varepsilon_{ij,k}\right)$$

$$\chi_{ij}^s = \frac{1}{2}\left(\theta_{i,j} + \theta_{j,i}\right) \tag{8}$$

$$\theta_i = \frac{1}{2}\left(\mathrm{curl}(u)\right)_i \tag{9}$$

In which u_i is the displacement vector, θ_i is the infinitesimal rotation vector, ε_{mm} is the dilatation strain and δ_{ij} is the kronecker delta. In addition, the classical stress tensor σ_{ij} and the higher-order stresses $p_i, \tau_{ijk}^{(1)}, m_{ij}^s$ can be given as:

$$\begin{aligned} \sigma_{ij} &= \lambda tr(\varepsilon)\delta_{ij} + 2\mu\varepsilon_{ij} \\ p_i &= 2\mu l_0^2 \gamma_i \\ \tau_{ijk}^{(1)} &= 2\mu l_1^2 \eta_{ijk}^{(1)} \\ m_{ij}^s &= 2\mu l_2^2 \chi_{ij}^s \end{aligned} \tag{10}$$

where l_0, l_1, l_2 denote the additional independent material length scale parameters associated with dilatation gradient, deviatoric stretch gradient and symmetric rotation gradient, respectively, which are assumed to be the same in this study.

By substituting Eq. (3) into Eq. (5), the non-zero components of the strain–displacement can be written as:

$$\boldsymbol{\varepsilon} = \begin{Bmatrix} \varepsilon_{xx} \\ \varepsilon_{yy} \\ \varepsilon_{xy} \end{Bmatrix} = \boldsymbol{\varepsilon}^0 + \bar{z}\boldsymbol{\kappa}, \boldsymbol{\varepsilon}^0 = \begin{Bmatrix} \varepsilon_{xx}^0 \\ \varepsilon_{yy}^0 \\ \varepsilon_{xy}^0 \end{Bmatrix} = \boldsymbol{\varepsilon}_l^0 + \boldsymbol{\varepsilon}_{nl}^0 \tag{11}$$

In which $\boldsymbol{\varepsilon}_l^0$, $\boldsymbol{\varepsilon}_{nl}^0$ and $\boldsymbol{\kappa}$ are linear strains vector, nonlinear strains vector and curvature strains vector, respectively and can be obtained as:

$$\boldsymbol{\varepsilon}_l^0 = \begin{Bmatrix} \frac{\partial u}{\partial x} \\ \frac{\partial v}{\partial y} \\ \frac{\partial u}{\partial y} + \frac{\partial v}{\partial x} \end{Bmatrix}, \quad \boldsymbol{\varepsilon}_{nl}^0 = \begin{Bmatrix} \frac{1}{2}\left(\frac{\partial w}{\partial x}\right)^2 \\ \frac{1}{2}\left(\frac{\partial w}{\partial y}\right)^2 \\ \frac{\partial w}{\partial x}\frac{\partial w}{\partial y} \end{Bmatrix} \tag{12}$$

and

$$\boldsymbol{\kappa} = \begin{Bmatrix} k_x \\ k_y \\ k_{xy} \end{Bmatrix} = \begin{Bmatrix} \frac{\partial \varphi_x}{\partial x} \\ \frac{\partial \varphi_y}{\partial y} \\ \frac{\partial \varphi_x}{\partial y} + \frac{\partial \varphi_y}{\partial x} \end{Bmatrix} \tag{13}$$

Similar to the above, the shear strains vector ε_s is also obtained by:

$$\boldsymbol{\varepsilon}_s = \begin{Bmatrix} \varepsilon_{yz} \\ \varepsilon_{xz} \end{Bmatrix} = \begin{Bmatrix} \varphi_y + \frac{\partial w}{\partial y} \\ \varphi_x + \frac{\partial w}{\partial x} \end{Bmatrix} \tag{14}$$

The components of infinitesimal rotation vector can be defined by substituting Eq. (3) into Eq. (9) as:

$$\boldsymbol{\theta} = \begin{Bmatrix} \theta_x \\ \theta_y \\ \theta_z \end{Bmatrix} = \frac{1}{2}\begin{Bmatrix} \frac{\partial w}{\partial y} - \varphi_y \\ -\frac{\partial w}{\partial x} + \varphi_x \\ \left(\frac{\partial v}{\partial x} - \frac{\partial u}{\partial y}\right) + \bar{z}\left(\frac{\partial \varphi_y}{\partial x} - \frac{\partial \varphi_x}{\partial y}\right) \end{Bmatrix} \tag{15}$$

The components of dilatation vector can also be expressed by putting Eqs. (12) -(14) and (15) into Eq. (6) as:

$$\boldsymbol{\gamma}=\begin{Bmatrix}\gamma_x\\ \gamma_y\\ \gamma_z\end{Bmatrix}=\boldsymbol{\gamma}_1+\bar{z}\boldsymbol{\gamma}_2;$$
$$\boldsymbol{\gamma}_1=\begin{Bmatrix}\dfrac{\partial^2 u}{\partial x^2}+\dfrac{\partial^2 v}{\partial xy}\\ \dfrac{\partial^2 v}{\partial y^2}+\dfrac{\partial^2 u}{\partial xy}\\ \dfrac{\partial \varphi_x}{\partial x}+\dfrac{\partial \varphi_y}{\partial y}\end{Bmatrix},\quad \boldsymbol{\gamma}_2=\begin{Bmatrix}\dfrac{\partial^2 \varphi_x}{\partial x^2}+\dfrac{\partial^2 \varphi_y}{\partial xy}\\ \dfrac{\partial^2 \varphi_y}{\partial y^2}+\dfrac{\partial^2 \varphi_x}{\partial xy}\\ 0\end{Bmatrix} \tag{16}$$

and by replacing Eqs. (12), (14) and (15) into Eq. (7), the components of deviatoric stretch gradient vector can be found as:

$$\boldsymbol{\eta}=\begin{Bmatrix}\eta^{(1)}_{xxx}\\ \eta^{(1)}_{yyy}\\ \eta^{(1)}_{zzz}\\ \eta^{(1)}_{xxy}\\ \eta^{(1)}_{xxz}\\ \eta^{(1)}_{yyx}\\ \eta^{(1)}_{yyz}\\ \eta^{(1)}_{xyz}\\ \eta^{(1)}_{zzx}\\ \eta^{(1)}_{zzy}\end{Bmatrix}=\boldsymbol{\eta}_1+\bar{z}\boldsymbol{\eta}_2;$$
$$\boldsymbol{\eta}_1=\frac{1}{15}\begin{Bmatrix}3\left(2\dfrac{\partial^2 u}{\partial x^2}-\dfrac{\partial^2 u}{\partial y^2}-2\dfrac{\partial^2 v}{\partial xy}\right)\\ 3\left(2\dfrac{\partial^2 v}{\partial y^2}-\dfrac{\partial^2 v}{\partial x^2}-2\dfrac{\partial^2 u}{\partial xy}\right)\\ 3\left(\dfrac{\partial^2 w}{\partial x^2}+\dfrac{\partial^2 w}{\partial y^2}+2\dfrac{\partial \varphi_x}{\partial x}+2\dfrac{\partial \varphi_y}{\partial y}\right)\\ \left(4\dfrac{\partial^2 v}{\partial x^2}+8\dfrac{\partial^2 u}{\partial xy}-3\dfrac{\partial^2 v}{\partial y^2}\right)\\ \left(8\dfrac{\partial \varphi_x}{\partial x}-2\dfrac{\partial \varphi_y}{\partial y}+4\dfrac{\partial^2 w}{\partial x^2}-\dfrac{\partial^2 w}{\partial y^2}\right)\\ \left(4\dfrac{\partial^2 u}{\partial y^2}+8\dfrac{\partial^2 v}{\partial xy}-3\dfrac{\partial^2 u}{\partial x^2}\right)\\ \left(8\dfrac{\partial \varphi_y}{\partial y}-2\dfrac{\partial \varphi_x}{\partial x}+4\dfrac{\partial^2 w}{\partial y^2}-\dfrac{\partial^2 w}{\partial x^2}\right)\\ 5\left(\dfrac{\partial^2 w}{\partial xy}+\dfrac{\partial \varphi_x}{\partial y}+\dfrac{\partial \varphi_y}{\partial x}\right)\\ -\left(3\dfrac{\partial^2 u}{\partial x^2}+2\dfrac{\partial^2 v}{\partial xy}+\dfrac{\partial^2 u}{\partial y^2}\right)\\ -\left(3\dfrac{\partial^2 v}{\partial y^2}+2\dfrac{\partial^2 u}{\partial xy}+\dfrac{\partial^2 v}{\partial x^2}\right)\end{Bmatrix};$$
$$\boldsymbol{\eta}_2=\frac{1}{15}\begin{Bmatrix}3\left(2\dfrac{\partial^2 \varphi_x}{\partial x^2}-\dfrac{\partial^2 \varphi_x}{\partial y^2}-2\dfrac{\partial^2 \varphi_y}{\partial xy}\right)\\ 3\left(2\dfrac{\partial^2 \varphi_y}{\partial y^2}-\dfrac{\partial^2 \varphi_y}{\partial x^2}-2\dfrac{\partial^2 \varphi_x}{\partial xy}\right)\\ 0\\ \left(8\dfrac{\partial^2 \varphi_x}{\partial xy}+4\dfrac{\partial^2 \varphi_y}{\partial x^2}-3\dfrac{\partial^2 \varphi_y}{\partial y^2}\right)\\ 0\\ \left(8\dfrac{\partial^2 \varphi_y}{\partial xy}+4\dfrac{\partial^2 \varphi_x}{\partial y^2}-3\dfrac{\partial^2 \varphi_x}{\partial x^2}\right)\\ 0\\ 0\\ -\left(3\dfrac{\partial^2 \varphi_x}{\partial x^2}+2\dfrac{\partial^2 \varphi_y}{\partial xy}+\dfrac{\partial^2 \varphi_x}{\partial y^2}\right)\\ -\left(3\dfrac{\partial^2 \varphi_y}{\partial y^2}+2\dfrac{\partial^2 \varphi_x}{\partial xy}+\dfrac{\partial^2 \varphi_y}{\partial x^2}\right)\end{Bmatrix} \tag{17}$$

It is worth noting that the equations $\eta^{(1)}_{xxy}=\eta^{(1)}_{xyx}=\eta^{(1)}_{yxx}$, $\eta^{(1)}_{yyx}=\eta^{(1)}_{yxy}=\eta^{(1)}_{xyy}$, $\eta^{(1)}_{xxz}=\eta^{(1)}_{xzx}=\eta^{(1)}_{zxx}$, $\eta^{(1)}_{yyz}=\eta^{(1)}_{yzy}=\eta^{(1)}_{zyy}$, $\eta^{(1)}_{zzx}=\eta^{(1)}_{zxz}=\eta^{(1)}_{xzz}$, $\eta^{(1)}_{zzy}=\eta^{(1)}_{zyz}=\eta^{(1)}_{yzz}$ and $\eta^{(1)}_{xyz}=\eta^{(1)}_{yzx}=\eta^{(1)}_{zxy}=\eta^{(1)}_{xzy}=\eta^{(1)}_{yxz}=\eta^{(1)}_{zyx}$ are established in the above relations. Finally, the components of symmetric rotation gradient vector can be obtained by substituting Eqs. (12), (14) and (15) into Eq. (8) as:

$$\boldsymbol{\chi}^s=\begin{Bmatrix}\chi^s_{xx}\\ \chi^s_{yy}\\ \chi^s_{zz}\\ \chi^s_{xy}\\ \chi^s_{xz}\\ \chi^s_{yz}\end{Bmatrix}=\boldsymbol{\chi}^s_1+\bar{z}\boldsymbol{\chi}^s_2;$$
$$\boldsymbol{\chi}^s_1=\frac{1}{2}\begin{Bmatrix}\dfrac{\partial^2 w}{\partial xy}-\dfrac{\partial \varphi_y}{\partial x}\\ \dfrac{\partial \varphi_x}{\partial y}-\dfrac{\partial^2 w}{\partial xy}\\ -\dfrac{\partial \varphi_x}{\partial y}+\dfrac{\partial \varphi_y}{\partial x}\\ \dfrac{1}{2}\left(\dfrac{\partial^2 w}{\partial y^2}-\dfrac{\partial^2 w}{\partial x^2}-\dfrac{\partial \varphi_y}{\partial y}+\dfrac{\partial \varphi_x}{\partial x}\right)\\ \dfrac{1}{2}\left(\dfrac{\partial^2 v}{\partial x^2}-\dfrac{\partial^2 u}{\partial xy}\right)\\ \dfrac{1}{2}\left(\dfrac{\partial^2 v}{\partial xy}-\dfrac{\partial^2 u}{\partial y^2}\right)\end{Bmatrix};$$
$$\boldsymbol{\chi}^s_2=-\frac{1}{4}\begin{Bmatrix}0\\ 0\\ 0\\ 0\\ \dfrac{\partial^2 \varphi_x}{\partial xy}-\dfrac{\partial^2 \varphi_y}{\partial x^2}\\ \dfrac{\partial^2 \varphi_x}{\partial y^2}-\dfrac{\partial^2 \varphi_y}{\partial xy}\end{Bmatrix} \tag{18}$$

By using Eq. (11), (18) and substituting them into Eq. (10), the classical stress tensor σ_{ij} and the higher-order stresses $p_i, \tau^{(1)}_{ijk}, m^s_{ij}$ can ultimately be obtained.

By knowing the stresses and strains as described above, the total potential energy of the FG micro-plate can be calculated. The total potential energy Π is equal to the summation of strain energy Π_S and potential energy of external loads Π_w. Since in the present paper, for the study of nonlinear bending analysis, the micro-plate is assumed to be under lateral pressure loads q_0 and for post-buckling analysis, it is under in-plane biaxial loads $N_x=\gamma_1 p$ and $N_y=\gamma_2 p$, so the potential energy of external loads can be calculated as follows:

$$\Pi_w=\int_A\left(N_x\left(\frac{\partial u}{\partial x}\right)+N_y\left(\frac{\partial v}{\partial y}\right)+q_0 w\right)dA \tag{19}$$

It should be noted that in the above equation, the assumption $\gamma_1=\gamma_2=1$ is considered in this study.

In order to obtain the nonlinear bending results, the in-plane biaxial loads are supposed to be zero (i.e. $N_x=N_y=0$) and the lateral pressure loads are also assumed to be zero (i.e.$q_0=0$) for post-buckling results. The strain energy of FG micro-plate Π_S can also be written as:

$$\Pi_S=\Pi_E+\Pi_{M\varsigma 1}+\Pi_{M\varsigma 2}+\Pi_{M\varsigma 3} \tag{20}$$

where $\Pi_E, \Pi_{M\varsigma 1}, \Pi_{M\varsigma 2}$ and $\Pi_{M\varsigma 3}$ are the strain energies correspond to the classical stresses, dilatation stresses,

deviatoric stretch stresses and the couple stresses, respectively, and are defined by using Eqs. (4), (11), (13), (14), (16), (17) and (18) as below.

$$\Pi_E = \frac{1}{2}\int_A \{\boldsymbol{F}^T\boldsymbol{\varepsilon}^0 + \boldsymbol{H}^T\kappa + \boldsymbol{Q}^T\boldsymbol{\varepsilon}_s\}\,dA \tag{21}$$

$$\Pi_{M\varsigma 1} = \frac{1}{2}\int_A \{\boldsymbol{P}^T\boldsymbol{\gamma}_1 + \boldsymbol{P}\boldsymbol{H}^T\boldsymbol{\gamma}_2\}\,dA \tag{22}$$

$$\Pi_{M\varsigma 2} = \frac{1}{2}\int_A \{\boldsymbol{T}^T\boldsymbol{\eta}_1 + \boldsymbol{T}\boldsymbol{H}^T\boldsymbol{\eta}_2\}\,dA \tag{23}$$

$$\Pi_{M\varsigma 3} = \frac{1}{2}\int_A \{\boldsymbol{S}^T\boldsymbol{\chi}_1^s + \boldsymbol{S}\boldsymbol{H}^T\boldsymbol{\chi}_2^s\}\,dA \tag{24}$$

where

$$\begin{aligned}
\boldsymbol{F} &= \begin{Bmatrix} F_{xx} \\ F_{yy} \\ F_{xy} \end{Bmatrix} = \int_{-\frac{h}{2}}^{\frac{h}{2}} \begin{Bmatrix} \sigma_{xx} \\ \sigma_{yy} \\ \sigma_{xy} \end{Bmatrix} d\bar{z}; \\
\boldsymbol{H} &= \begin{Bmatrix} H_{xx} \\ H_{yy} \\ H_{xy} \end{Bmatrix} = \int_{-\frac{h}{2}}^{\frac{h}{2}} \begin{Bmatrix} \sigma_{xx} \\ \sigma_{yy} \\ \sigma_{xy} \end{Bmatrix} \bar{z}\,d\bar{z}; \\
\boldsymbol{Q} &= \begin{Bmatrix} Q_x \\ Q_y \end{Bmatrix} = k_s \int_{-\frac{h}{2}}^{\frac{h}{2}} \begin{Bmatrix} \sigma_{xz} \\ \sigma_{yz} \end{Bmatrix} d\bar{z}
\end{aligned} \tag{25}$$

$$\begin{aligned}
\boldsymbol{P} &= \begin{Bmatrix} P_x \\ P_y \\ P_z \end{Bmatrix} = \int_{-\frac{h}{2}}^{\frac{h}{2}} \begin{Bmatrix} p_x \\ p_y \\ p_z \end{Bmatrix} d\bar{z}; \\
\boldsymbol{PH} &= \begin{Bmatrix} PH_x \\ PH_y \\ 0 \end{Bmatrix} = \int_{-\frac{h}{2}}^{\frac{h}{2}} \begin{Bmatrix} p_x \\ p_y \\ 0 \end{Bmatrix} \bar{z} d\bar{z}
\end{aligned} \tag{26}$$

$$\boldsymbol{T} = \begin{Bmatrix} T_{xxx} \\ T_{yyy} \\ T_{zzz} \\ T_{xxy} \\ T_{xxz} \\ T_{yyx} \\ T_{yyz} \\ T_{xyz} \\ T_{zzx} \\ T_{zzy} \end{Bmatrix} = \int_{-\frac{h}{2}}^{\frac{h}{2}} \begin{Bmatrix} \tau_{xxx}^{(1)} \\ \tau_{yyy}^{(1)} \\ \tau_{zzz}^{(1)} \\ \tau_{xxy}^{(1)} \\ \tau_{xxz}^{(1)} \\ \tau_{yyx}^{(1)} \\ \tau_{yyz}^{(1)} \\ \tau_{xyz}^{(1)} \\ \tau_{zzx}^{(1)} \\ \tau_{zzy}^{(1)} \end{Bmatrix} d\bar{z}\,; \tag{27}$$

$$\boldsymbol{TH} = \begin{Bmatrix} TH_{xxx} \\ TH_{yyy} \\ 0 \\ TH_{xxy} \\ 0 \\ TH_{yyx} \\ 0 \\ 0 \\ TH_{zzx} \\ TH_{zzy} \end{Bmatrix} = \int_{-\frac{h}{2}}^{\frac{h}{2}} \begin{Bmatrix} \tau_{xxx}^{(1)} \\ \tau_{yyy}^{(1)} \\ 0 \\ \tau_{xxy}^{(1)} \\ 0 \\ \tau_{yyx}^{(1)} \\ 0 \\ 0 \\ \tau_{zzx}^{(1)} \\ \tau_{zzy}^{(1)} \end{Bmatrix} \bar{z}\,d\bar{z}$$

$$\begin{aligned}
\boldsymbol{S} &= \begin{Bmatrix} S_{xx} \\ S_{yy} \\ S_{zz} \\ S_{xy} \\ S_{xz} \\ S_{yz} \end{Bmatrix} = \int_{-\frac{h}{2}}^{\frac{h}{2}} \begin{Bmatrix} m_{xx}^s \\ m_{yy}^s \\ m_{zz}^s \\ m_{xy}^s \\ m_{xz}^s \\ m_{yz}^s \end{Bmatrix} d\bar{z}; \\
\boldsymbol{SH} &= \begin{Bmatrix} 0 \\ 0 \\ 0 \\ 0 \\ SH_{xz} \\ SH_{yz} \end{Bmatrix} = \int_{-\frac{h}{2}}^{\frac{h}{2}} \begin{Bmatrix} 0 \\ 0 \\ 0 \\ 0 \\ m_{xz}^s \\ m_{yz}^s \end{Bmatrix} \bar{z}\,d\bar{z}
\end{aligned} \tag{28}$$

Parameter k_s represents the shear correction factor.

So far, all the required relations have been extracted, and the only unknowns left in the functional of the total potential energy are the displacement fields. Therefore, it is necessary to calculate the total potential energy by estimating the displacement fields in the Ritz technique. For this purpose, the essential boundary conditions of the problem must be specified. This work includes three different types of boundary conditions as follows.

a) FG micro-plates with all simply-supported edges (SSSS):

$$\begin{aligned}
&u|_{x=0,a} = 0 \qquad u|_{y=0,b} = 0, \\
&v|_{x=0,a} = 0, \qquad v|_{y=0,b} = 0 \\
&u|_{x=0} = -u_c \qquad u|_{x=a} = u_c, v|_{y=0} = -v_c \\
&\qquad v|_{y=b} = v_c \quad \text{(for post-buckling)} \\
&w|_{x=0,a} = 0, \qquad w|_{y=0,b} = 0, \\
&\varphi_x|_{y=0,b} = 0, \quad \varphi_y\big|_{x=0,a} = 0
\end{aligned} \tag{29}$$

b) FG micro-plates with simply-supported conditions on edges $x = 0, a$ and clamped conditions on edges $y = 0, b$ (CSCS):

$$\begin{aligned}
&u|_{x=0,a} = 0 \qquad u|_{y=0,b} = 0, \\
&v|_{x=0,a} = 0, \qquad v|_{y=0,b} = 0 \\
&u|_{x=0} = -u_c \qquad u|_{x=a} = u_c, \; v|_{y=0} = -v_c \\
&\qquad v|_{y=b} = v_c \quad \text{(for post-buckling)} \\
&w|_{x=0,a} = 0, \qquad w|_{y=0,b} = 0, \\
&\varphi_x|_{y=0,b} = 0, \; \varphi_y\big|_{x=0,a} = 0, \varphi_y\big|_{y=0,b} = 0
\end{aligned} \tag{30}$$

$$\begin{aligned}
&u|_{x=0,a} = 0 \qquad u|_{y=0,b} = 0, \\
&v|_{x=0,a} = 0, \qquad v|_{y=0,b} = 0 \\
&u|_{x=0} = -u_c \qquad u|_{x=a} = u_c, \\
&v|_{y=0} = -v_c \qquad v|_{y=b} = v_c \;\text{(for post-buckling)} \\
&w|_{x=0,a} = 0, \qquad w|_{y=0,b} = 0 \\
&\varphi_x|_{x=0,a} = 0, \qquad \varphi_x|_{y=0,b} = 0, \\
&\varphi_y\big|_{x=0,a} = 0, \qquad \varphi_y\big|_{y=0,b} = 0
\end{aligned} \tag{31}$$

c) FG micro-plates with all clamped edges (CCCC):

For both bending and post-buckling analyzes, all the conditions mentioned in the above relations are met, except for normal in-plane conditions (i.e. longitudinally for u or laterally for v), in which the edges are allowed to move but remain straight.

Given that the Riley-Ritz technique is used in this study,

the estimated displacement fields should meet the above essential boundary conditions. Displacement fields are estimated by Legendre's basic functions $P_n(x)$ or Legendre's polynomials, which are powerful tools for functions approximation. These polynomials are obtained by solving the following Legendre differential equation:

$$\frac{d}{dx}\left[(1-x^2)\frac{d}{dx}P_n(x)\right]+n(n+1)P_n(x)=0 \tag{32}$$

Also, Legendre polynomials satisfy the three-term recursive relations as:

$$P_{n+1}(x)=\frac{2n+1}{n+1}xP_n(x)-\frac{n}{n+1}P_{n-1}(x) \tag{33}$$

where $P_0(x)=1$ and $P_1(x)=x$. So the displacement fields can be approximated as (Ghannadpour *et al*. 2019a, b):

$$\tau(x,y)=\mathbb{B}_\tau(x,y)\sum_{m=1}^{N_t}\sum_{n=1}^{N_t}\delta_{mn}^{\tau}P_{m-1}\left(\frac{x}{a}\right)P_{n-1}\left(\frac{y}{b}\right)+f_\tau(x,y)\delta_c^{\tau} \tag{34}$$

where $\tau\in\{u,v,w,\varphi_x,\varphi_y\}$ is a displacement field. N_t is the number of terms in series expansion which is chosen the same for all displacement fields and m and n are positive integers. The coefficients δ_{mn}^{τ} and δ_c^{τ} are the Ritz unknown coefficients of the problem and the latter is for satisfying the straight conditions mentioned before.

Therefore, the boundary function $f_\tau(x,y)$ is also chosen to ensure the satisfaction of the straight boundary conditions of the micro-plates. Since this specified boundary condition is only related to the in-plane displacement fields, the value of this function is zero for out-of-plane displacement functions. The so-called boundary function $\mathbb{B}_\tau(x,y)$ is taken to ensure the fulfillment of the essential boundary conditions. It can be written as (Ghannadpour and shakeri 2018):

$$\mathbb{B}_\tau(x,y)=\prod_{\beta=1,2}\left(1+(-1)^{\beta-1}\left(\frac{x}{a}\right)\right)^{\mu_\beta^{\tau}}\prod_{\beta=3,4}\left(1+(-1)^{\beta-1}\left(\frac{y}{b}\right)\right)^{\mu_\beta^{\tau}} \tag{35}$$

In which β represents the edge number and the exponents μ_β^{τ} can take the value 0 for free condition and the value 1 according to the conditions of held (or straight) for each displacement field $\tau\in\{u,v,w,\varphi_x,\varphi_y\}$. By adopting the displacement fields as above, the total potential energy of the micro-plate can be rewritten in a matrix form by using the Hessian technique:

$$\Pi=-\boldsymbol{d}^T\boldsymbol{V}_w+\frac{1}{2}\boldsymbol{d}^T\boldsymbol{K}_0\boldsymbol{d}+\frac{1}{6}\boldsymbol{d}^T\boldsymbol{K}_1\boldsymbol{d}+\frac{1}{12}\boldsymbol{d}^T\boldsymbol{K}_2\boldsymbol{d} \tag{36}$$

In which $\boldsymbol{V}_w$ represents a vector of constants, including the effects of the applied loads. The vector $\boldsymbol{d}$ contains the unknown of the problems. Stiffness matrices of the micro-plate are represented by $\boldsymbol{K}_0,\boldsymbol{K}_1$ and $\boldsymbol{K}_2$ matrices whose coefficients are constant, linear and quadratic functions of the unknowns, respectively. The nonlinear equilibrium equations of the functionally-graded micro-plate can be obtained by using the principle of minimum total potential energy. In other words, partial differentiations of the total potential energy with respect to the unknowns give a set of nonlinear equilibrium equations as

$$-\boldsymbol{V}_w+\left(\boldsymbol{K}_0+\frac{1}{2}\boldsymbol{K}_1+\frac{1}{3}\boldsymbol{K}_2\right)\boldsymbol{d}=0 \tag{37}$$

To solve the above nonlinear algebraic equations, the Newton-Raphson technique is employed and a relevant convergence criterion in this study is defined based on the vector containing the unknown coefficients ($\boldsymbol{d}$). The iterative process is repeated until it is satisfied by the following conditions.

$$\sqrt{\frac{\sum\Delta\boldsymbol{d}_i^2}{\sum\Delta\boldsymbol{d}_{i+1}^2}}<10^{-4} \tag{38}$$

where i is the iteration counter in Newton-Raphson technique. Once the nonlinear equilibrium equations are solved and the unknown coefficients are identified, it becomes possible to calculate the displacements, strains and stresses at any point in the micro-plate.

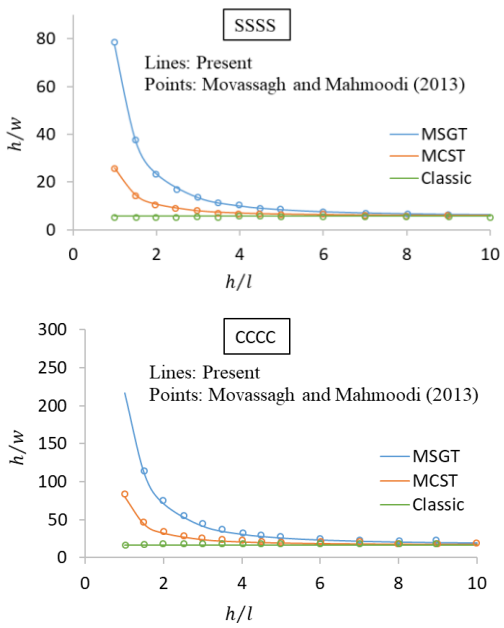

Fig. 2 Comparison of three different theories versus thickness of FG micro-plates for boundary conditions SSSS and CCCC

3. Numerical results and discussion

3.1 Validation of the results

To validate the formulation presented in this study, the bending results obtained are compared with those presented by Movassagh and Mahmoodi (2013) in Fig. 2. The results shown in Fig. 2 are for micro-plates with SSSS and CCCC boundary conditions, both represent changes in the center deflection of the micro-plate in terms of the length scale parameter. As can be seen, the results for all three theories,

Table 1 Dimensionless deflections of simply-supported square FG micro-plates

k	l/h	$a/h=5$			$a/h=10$			$a/h=20$		
		Thai and Choi (2013)	MCST	MSGT	Thai and Choi (2013)	MCST	MSGT	Thai and Choi (2013)	MCST	MSGT
0	0	0.5147	0.5183	0.5183	0.4415	0.4451	0.4451	0.4232	0.4268	0.4268
	0.2	0.4479	0.4515	0.3678	0.3844	0.3876	0.2989	0.3684	0.3716	0.2815
	0.4	0.3250	0.3279	0.2233	0.2775	0.2799	0.1587	0.2655	0.2678	0.1414
	0.6	0.2268	0.2289	0.1537	0.1907	0.1922	0.0966	0.1814	0.1829	0.0793
	0.8	0.1631	0.1647	0.1151	0.1335	0.1346	0.0674	0.1259	0.1270	0.0507
	1	0.1230	0.1225	0.0901	0.0972	0.0980	0.0515	0.0906	0.0913	0.0357
1	0	1.1536	1.1622	1.1622	1.0205	1.0291	1.0291	0.9873	0.9959	0.9959
	0.2	0.9685	0.9763	0.6900	0.8567	0.8640	0.5708	0.8286	0.8358	0.5412
	0.4	0.6599	0.6657	0.4087	0.5798	0.5847	0.2937	0.5595	0.5643	0.2633
	0.6	0.4395	0.4436	0.2798	0.3790	0.3822	0.1767	0.3636	0.3667	0.1459
	0.8	0.3073	0.3102	0.2094	0.2573	0.2594	0.1228	0.2445	0.2465	0.0927
	1	0.2279	0.2302	0.1639	0.1838	0.1853	0.0938	0.1838	0.1739	0.0652
10	0	2.6273	2.6458	2.6458	2.2247	2.2431	2.2431	2.1240	2.1425	2.1425
	0.2	2.3127	2.3309	1.7120	1.9593	1.9757	1.3524	1.8705	1.8868	1.2634
	0.4	1.7138	1.7293	1.1287	1.4461	1.4583	0.7871	1.3781	1.3901	0.6978
	0.6	1.2163	1.2283	0.8086	1.0116	1.0202	0.5018	0.9591	0.9674	0.4106
	0.8	0.8841	0.8933	0.6168	0.7171	0.7232	0.3582	0.6740	0.6798	0.2685
	1	0.6710	0.6783	0.4869	0.5263	0.5308	0.2773	0.4888	0.4930	0.1917

the modified strain gradient theory (MSGT), the modified couple stress theory (MCST) and the classical theory are calculated and compared with Movassagh and Mahmoodi (2013). It is noted that the values of material properties, loading and geometry are also adapted from the same reference as $E = 1.44GPa,\ \nu = 0.38,\ l = l_0 = l_1 = l_2 = 17.6\mu m, q_0 = 1000N/m^2$ and $a = 50h$. As can be observed, the results are in excellent agreement with the results given by Movassagh and Mahmoodi (2013). It should be emphasized that in a convergence study for both nonlinear bending and post-buckling results, it is found that 4 terms $(N_t = 4)$ in each displacement field and for each direction are sufficient to obtain converged results.

In addition, dimensionless central deflections $\bar{w}$ of simply-supported square FG micro-plates based on the modified couple stress theory are provided in Table 1 and compared to those presented by Thai and Choi (2013). The results were obtained by the assumptions of $E_c = 14.4\ GPa, E_m = 1.44\ GPa, \nu = 0.38$ and $h = 17.6\mu m$ under the lateral pressure loads of $q_0 = 1N/m^2$. The dimensionless central deflections $\bar{w}$ has been calculated by $\frac{100E_m h^3}{q_0 a^4}\ w\left(\frac{a}{2}, \frac{b}{2}\right)$. As can be seen, the results of this study are very similar to those of Thai and Choi (2013) and it is noted that the results based on the modified strain gradient theory are also determined similarly and tabulated in Table1.

To provide the results in the following, all curves and graphs are presented in two sections of nonlinear bending and post-buckling for FG micro-plates. All responses for each analysis are obtained and presented using all three theories of modified strain gradient theory, modified couple stress theory and classical theory with different boundary conditions. The material properties from now on are assumed to be $E_c = 14.4\ GPa,\ E_m = 1.44\ GPa,\ \nu = 0.38$ and $l = l_0 = l_1 = l_2 = 17.6\mu m$ and the shear correction factor is taken to be $k_s = 5/6$. The following dimensionless parameters are also introduced for presenting

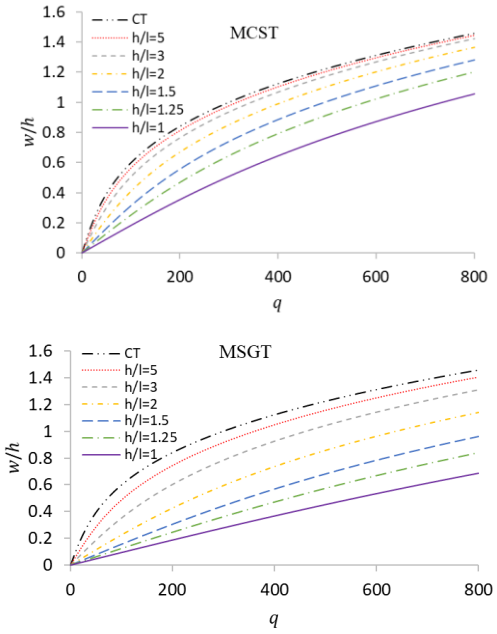

Fig. 3 Effect of thickness to length scale parameter on nonlinear bending of FG micro-plates for SSSS boundary conditions

the results.

$$N = \frac{pa^2}{E_m h^3}, q = \frac{q_0 a^4}{E_m h^4} \tag{39}$$

3.2 Nonlinear bending results

As mentioned before, at first, the results correspond to the nonlinear bending analysis are obtained and presented. The results related to modified strain gradient theory are distinguished by the abbreviation MSGT and the results related to modified couple stress theory are distinguished by

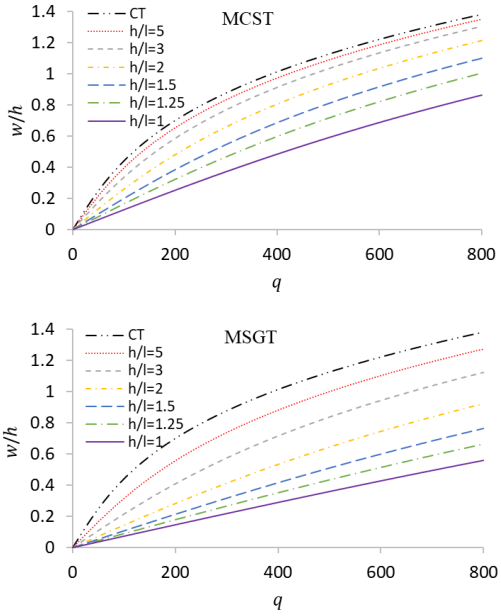

Fig. 4 Effect of thickness to length scale parameter on nonlinear bending of FG micro-plates for CSCS boundary conditions

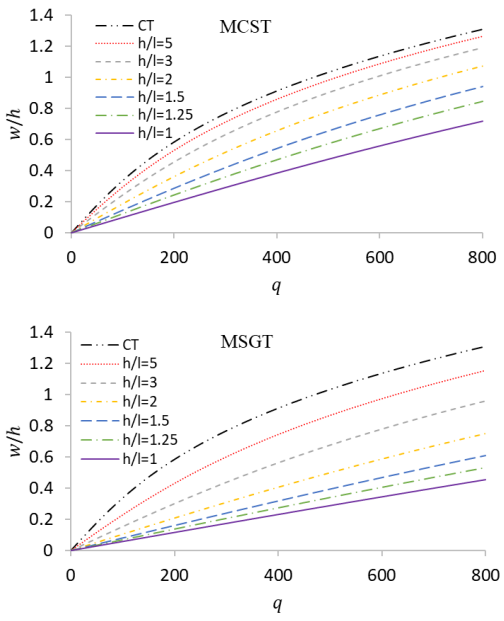

Fig. 5 Effect of thickness to length scale parameter on nonlinear bending FG micro-plates for CCCC boundary conditions

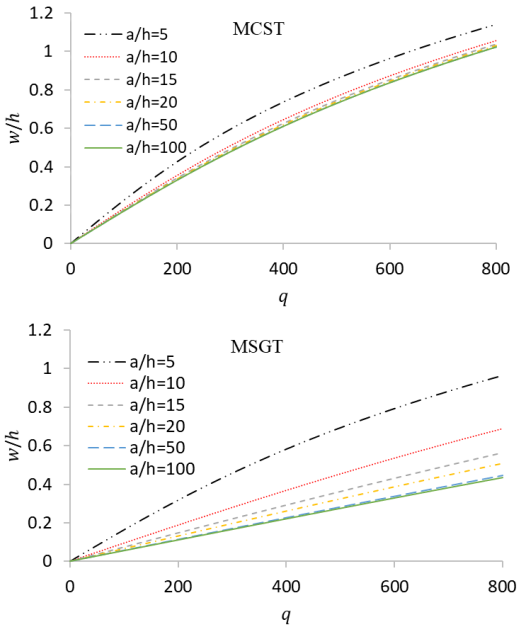

Fig. 6 Effect of length to thickness ratio on nonlinear bending of FG micro-plates for SSSS boundary conditions

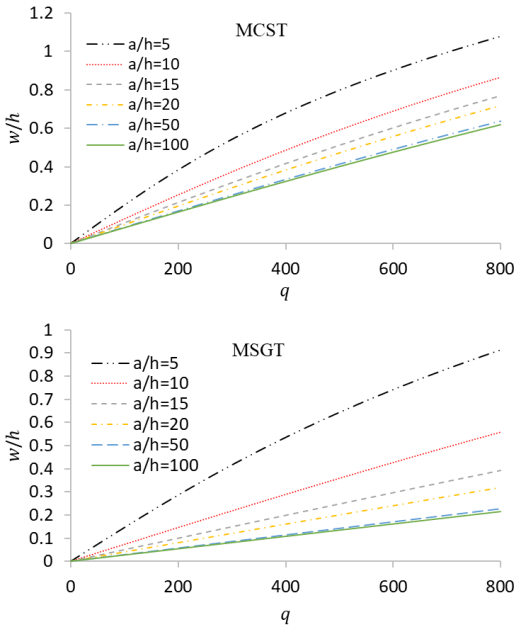

Fig. 7 Effect of length to thickness ratio on nonlinear bending of FG micro-plates for CSCS boundary conditions

the term MCST in figures.

Figs. 3-5 illustrate the effect of thickness to length scale parameter ratio h/l with SSSS, CSCS, and CCCC boundary conditions. The results were obtained by assuming $k = 1$ and $a / h = 10$. It is apparent from the figures that the classical theory (i.e. CT, $l = 0$) estimates higher dimensionless deflections than MCST and MSGT. With increasing h/l, MSGT and MCST results tend to those of their classical states. It can also be seen that the size effect depends on the boundary conditions, so it becomes more significant when the boundary conditions become stiffer.Figs. 6-8 show the effect of length to thickness ratio on nonlinear bending responses of FG micro-plates when they have $k = 1$ and $h/l = 1$. As expected, for both MSGT and MCST, the dimensionless deflection decreases with increasing length to thickness ratio, however, the MSGT again estimates lower values for deflection.

The impact of material gradient index on the nonlinear bending response of the FG micro-plates has been investigated in Figs. 9-11 for both MCST and MSGT and

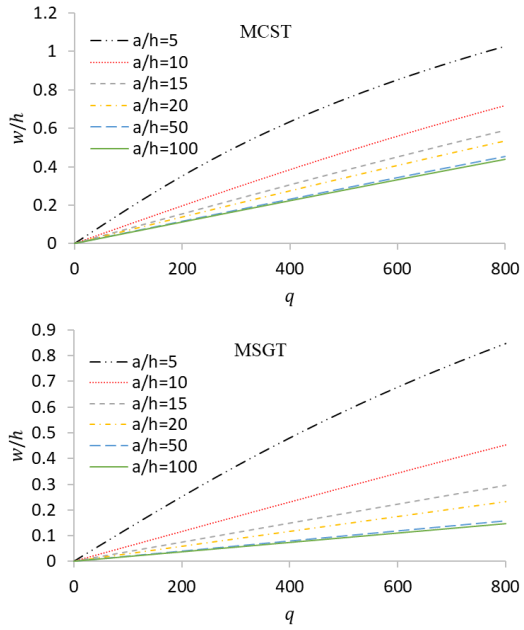

Fig. 8 Effect of length to thickness ratio on nonlinear bending of FG micro-plates for CCC boundary conditions

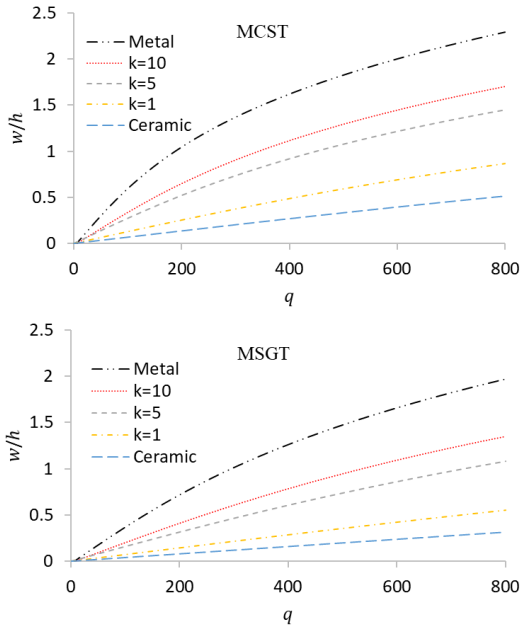

Fig. 10 Effect of material gradient index on nonlinear bending of FG micro-plates for CSCS boundary conditions

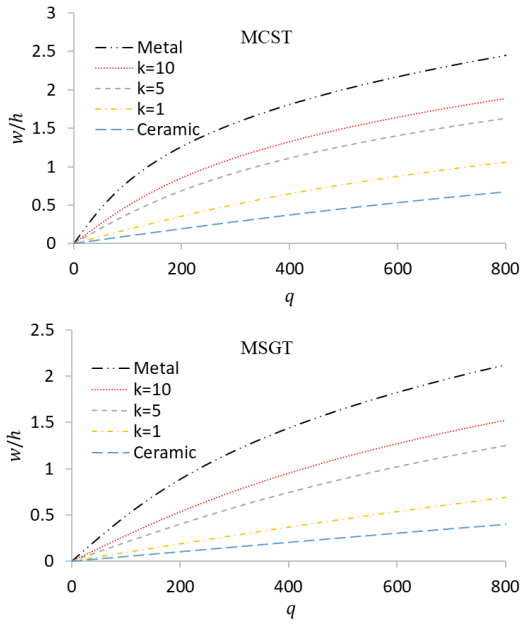

Fig. 9 Effect of material gradient index on nonlinear bending of FG micro-plates for SSSS boundary conditions

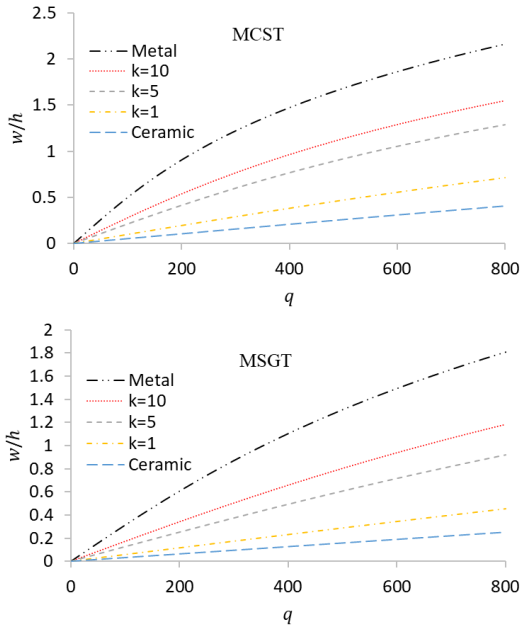

Fig. 11 Effect of material gradient index on nonlinear bending of FG micro-plates for CCCC boundary conditions

for mentioned boundary conditions. As can be seen, by increasing the material gradient index of the micro-plates, dimensionless deflection gets larger. As expected, metal curves have the highest values of dimensionless deflection, while ceramic curves have the smallest values due to their modulus of elasticity. Also, this behavior is seen in all three types of boundary conditions, but as expected, as the boundary conditions become stiffer, the amount of deflection decreases. It is noted that the results were obtained for the plates with assumptions of $h/l = 1$ and $a/h = 10$.

For a better and clearer comparison, the results of all three theories are shown in Fig. 12. These results are calculated and presented for simply-supported FG micro-plate with $a/h = 10$, $h/l = 1$, $k = 1$, and $a/b = 1$. As mentioned earlier, the results of MSGT, due to having three parameters of length scale, have less deflection compared to the results of MCST, and the classical theory predicts larger values because it does not take length scale effect into account.

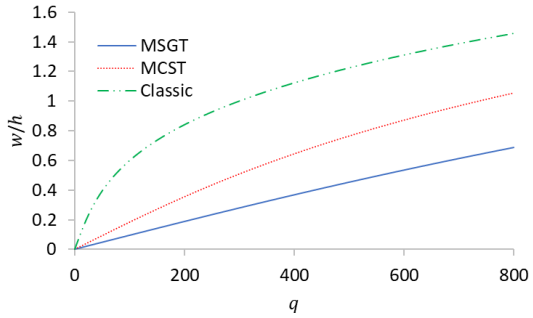

Fig. 12 Comparison between MSGT, MCST and classic theory results in nonlinear bending of FG micro-plate for SSSS boundary conditions

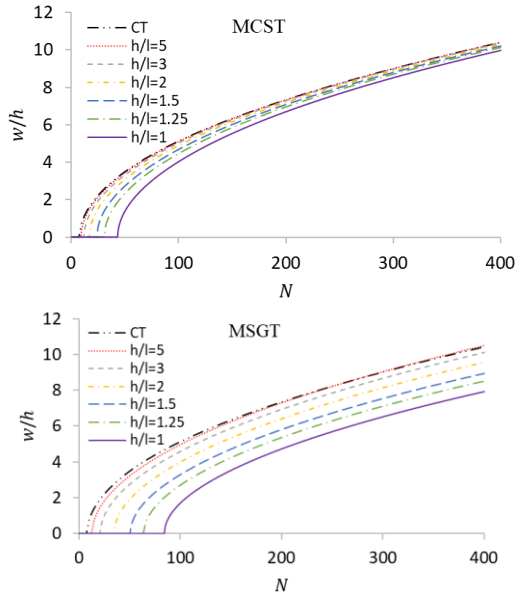

Fig. 13 Effect of thickness to length scale parameter on post-buckling behavior of FG micro-plates for SSSS boundary conditions

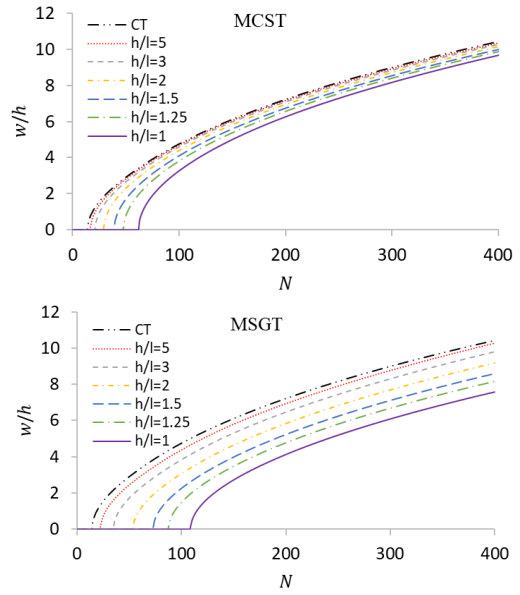

Fig. 14 Effect of thickness to length scale parameter on post-buckling behavior of FG micro-plates for CSCS boundary conditions

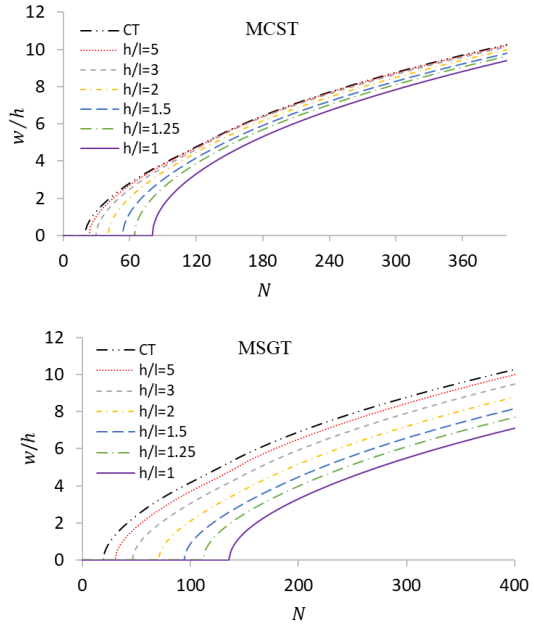

Fig. 15 Effect of thickness to length scale parameter on post-buckling behavior of FG micro-plates for CCCC boundary conditions

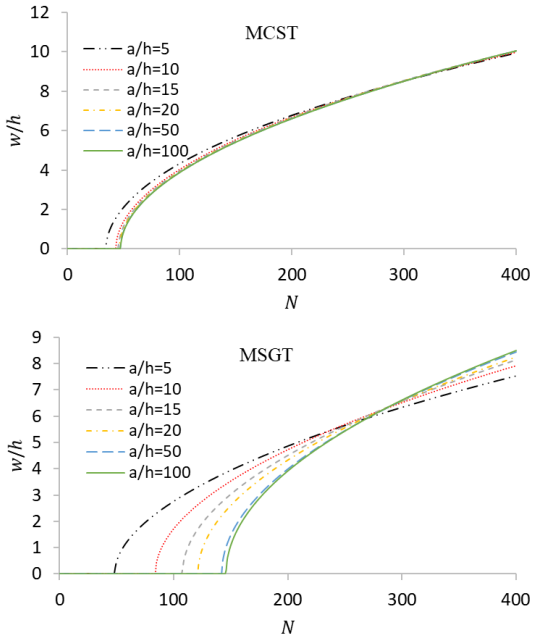

Fig. 16 Effect of length to thickness ratio on post-buckling behavior of FG micro-plates for SSSS boundary conditions

3.3 Post-buckling results

Similar to the previous section, post-buckling responses of FG micro-plates are presented in this section. All the assumptions in the analysis, boundary conditions and other parameters are the same as in the previous section, but instead of applying lateral pressure load q_0, biaxial in-plane loading are applied to the physical neutral plane in equal amounts.

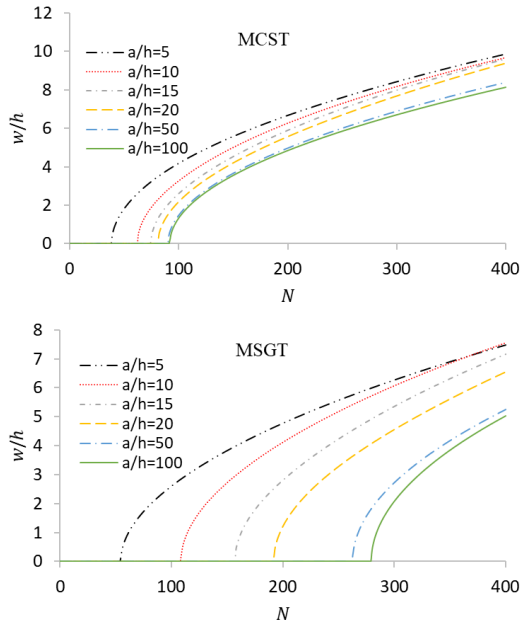

Fig. 17 Effect of length to thickness ratio on post-buckling behavior of FG micro-plates for CSCS boundary conditions

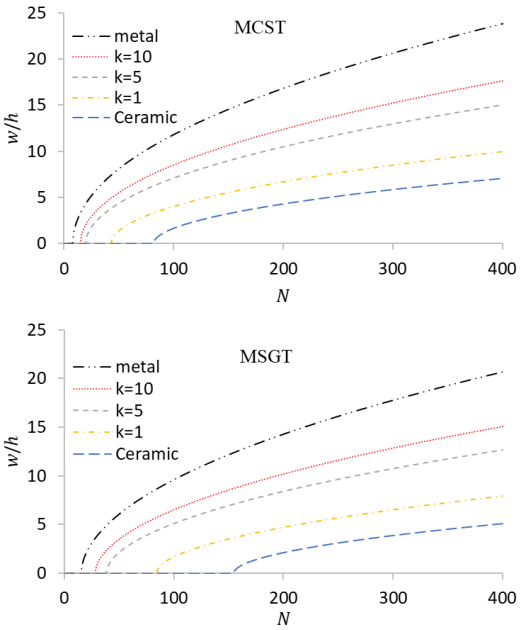

Fig. 19 Effect of material gradient index on post-buckling behavior of FG micro-plates for SSSS boundary conditions

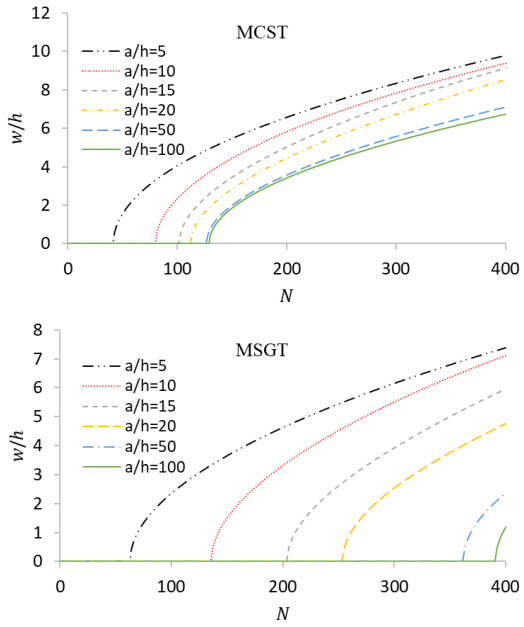

Fig. 18 Effect of length to thickness ratio on post-buckling behavior of FG micro-plates for CCCC boundary conditions

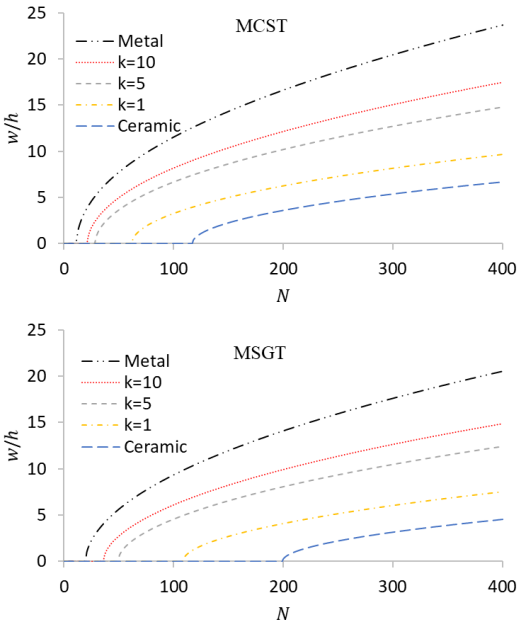

Fig. 20 Effect of material gradient index on post-buckling behavior of FG micro-plates for CSCS boundary conditions

Figs. 13-15 illustrate the effect of thickness to the length scale parameter ratio on post-buckling behavior of FG micro-plates with $k = 1$ and $a/h = 10$. These figures show how the dimensionless deflection increases with increasing the h/l (at specified loads) while the buckling load decreases. Hence, the CT $(l = 0)$ is characterized by the lowest buckling load. Moreover, the gap between the curves becomes smaller as h/l grows, which implies that the effects of the length scale are less pronounced when the amount of applied loads increases.

In order to complete the sensitivity studies and analyzes, although the conclusions were predictable, the results of post-buckling behavior of square FG micro-plates with different values of length to thickness ratio and for each type of boundary conditions are obtained and displayed in Figs. 16-18. These results were obtained for FG micro-plates with $k = 1$ and $h/l = 1$.

As it can be observed from these figures, the non-dimensional buckling load N_{cr} increases with increasing length to thickness ratio of the micro-plates, and this may

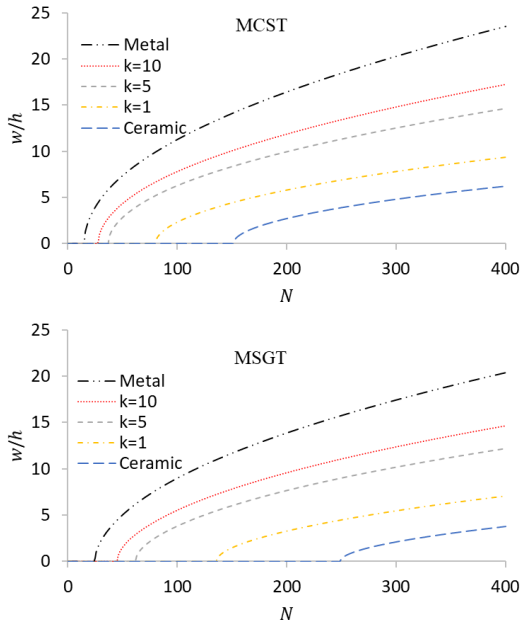

Fig. 21 Effect of material gradient index on post-buckling behavior of FG micro-plates for CCCC boundary conditions

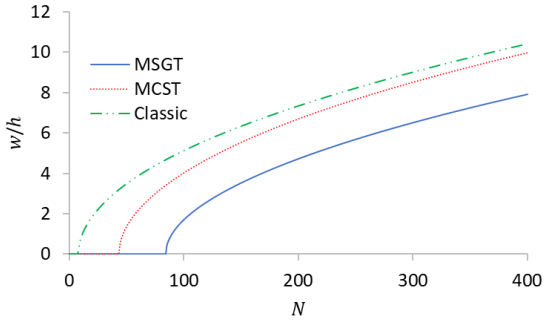

Fig. 22 Comparison between MSGT, MCST and classic theory in nonlinear post-buckling of a FG micro-plate with SSSS boundary conditions

be different from what is in mind. However, it should be noted that the actual buckling load decreases with increasing this ratio (i.e., increasing the length to thickness, which leads to a thinner plate), but due to the type of dimensionless formula selected in this paper (i.e., Eq. (34)), this trend occurs for dimensionless buckling load.

In Figs. 19-21, the effect of material gradient index is shown on post-buckling deflections of FG micro-plates for MSGT, MCST, and CT under SSSS, CSCS and CCCC boundary conditions, respectively. These responses were also obtained for FG plates with $h/l = 1, a/h = 10$. According to these figures, by increasing the value of material gradient index from zero to infinity and changing the composition of the material from pure ceramic to pure metal in the direction of thickness, the dimensionless buckling load decreases and due to the decrease in modulus of elasticity, the value of deflection also increases at specified loads.

Similar to previous section for nonlinear bending results, in order to better comparison, the results of all three theories have been shown in Fig. 22. These results are presented for a simply-supported FG micro-plate with $a/h = 10$, $h/l = 1$, $k = 1$, and $a/b = 1$. It is seen that the considering the length scale parameters increase the magnitude of buckling loads. In other words, the inclusion of the length scale effect will increase stiffness of the FG micro-plates, and therefore, leads to an increase in buckling loads. Hence, the size effect provides the FG micro-plate additional stiffness which cannot be neglected in the analysis of micro-structures.

It should be emphasized that in all post-buckling results, buckling loads and bifurcation points are observed, and this is due to the application of loads to the physical neutral plane, which eliminates the effects of the coupling matrix.

4. Conclusions

In this study, the size-dependent nonlinear bending and post-buckling behavior of functionally graded micro-plates were developed using the modified strain gradient theory. Further, the fundamental equations were formulated based on the first-order shear deformation theory and von-Karman assumptions. Minimizing the total potential energy was considered to obtain the plate equilibrium equations and solved using the Newton-Raphson technique. The Ritz method and Legendre polynomials were also used to approximate displacement fields. The present theory contains three length-scale parameters into the governing equations. The modified couple stress theory (MCST) and the classical theory (CT) were studied by ignoring the constants of two and three length scale parameters into the numerical results, respectively. In order to discard the bending-extensional coupling matrix, loads were applied to the physical neutral plane to observe the effects of different theories on buckling loads. The accuracy of this paper was examined by performing comparisons and convergence studies. By considering the thickness to length scale ratio, the length to thickness parameter, and the material gradient index, the nonlinear bending and post-buckling responses of the FG micro-plates were also calculated for three type of boundary conditions. Finally, it was found that the number of length scale parameters is very influential in the nonlinear analysis of micro-structures, which made MSGT be more accurate than MCST and CT. The size effect was most evident when the length scale parameter of the FG micro-plates was closer to the thickness. In general, h/l could be ignored if it exceeded a certain value. As a result, it was seen that the classical theories had lowest critical buckling load and the largest deflection in post-buckling stage. It means that the inclusion of the length scale effect will increase stiffness of the FG micro-plates, and therefore, leads to an increase in buckling loads. Hence, it was concluded that the size effect provides the FG micro-plate additional stiffness which cannot be neglected in the analysis of micro-structures.

References

Akbas, S.D. (2018), “Forced vibration analysis of cracked

functionally graded microbeams", *Adv. Nano Res.*, **6**(1), 39-55. http://doi.org/10.12989/anr.2018.6.1.039.

Akgöz, B. and Civalek, Ö. (2013), "Buckling analysis of functionally graded microbeams based on the strain gradient theory", *Acta Mechanica*, **224**(9), 2185-2201. https://doi.org/10.1007/s00707-013-0883-5.

Alinia, M.M. and Ghannadpour, S.A.M. (2009), "Nonlinear analysis of pressure loaded FGM plates", *Compos. Struct.*, **88**(3), 354-359. https://doi.org/10.1016/j.compstruct.2008.04.013.

Ansari, R., Faghih Shojaei, M., Shakouri, A.H. and Rouhi, H. (2016), "Nonlinear bending analysis of first-order shear deformable microscale plates using a strain gradient quadrilateral element", *J. Comput. Nonlinear Dyn.*, **11**(5). https://doi.org/10.1115/1.4032552.

Ansari, R., Gholami, R., Shojaei, M.F., Mohammadi, V. and Darabi, M.A. (2015), "Size-dependent nonlinear bending and postbuckling of functionally graded Mindlin rectangular microplates considering the physical neutral plane position", *Compos. Struct.*, **127**, 87-98. https://doi.org/10.1016/j.compstruct.2015.02.082.

Asghari, M., Rahaeifard, M., Kahrobaiyan, M.H. and Ahmadian, M.T. (2011), "The modified couple stress functionally graded Timoshenko beam formulation", *Mater. Des.*, **32**(3), 1435-1443. https://doi.org/10.1016/j.matdes.2010.08.046.

Avey, M., Fantuzzi, N., Sofiyev, A.H. and Kuruoglu, N. (2021), "Nonlinear vibration of multilayer shell-type structural elements with double curvature consisting of CNT patterned layers within different theories", *Compos. Struct.*, **275**, 114401. https://doi.org/10.1016/j.compstruct.2021.114401.

Bacciocchi, M., Fantuzzi, N., Luciano, R. and Tarantino, A.M. (2021), "Linear eigenvalue analysis of laminated thin plates including the strain gradient effect by means of conforming and nonconforming rectangular finite elements", *Comput. Struct.*, **257**, 106676. https://doi.org/10.1016/j.compstruc.2021.106676.

Bensaid, I., Bekhadda, A. and Kerboua, B. (2018), "Dynamic analysis of higher order shear-deformable nanobeams resting on elastic foundation based on nonlocal strain gradient theory", *Adv. Nano Res.*, **6**(3), 279-198. http://doi.org/10.12989/anr.2018.6.3.279.

Dehshahri, K., Nejad, M.Z., Ziaee, S., Niknejad, A. and Hadi, A. (2020), "Free vibrations analysis of arbitrary three-dimensionally FGM nanoplates", *Adv. Nano Res.*, **8**(2), 115-134. https://doi.org/10.12989/anr.2020.8.2.115.

Eringen, A.C. (1966), "Linear theory of micropolar elasticity", *J. Math. Mech.*, 909-923. https://www.jstor.org/stable/24901442.

Eringen, A.C. (1967), "Theory of micropolar plates", *Zeitschrift für Angewandte Mathematik und Physik ZAMP*, **18**(1), 12-30. https://doi.org/10.1007/BF01593891.

Fantuzzi, N., DENİZ, A., Kuruoglu, N. and Sofiyev, A.H. (2021), "Modeling and solution of large amplitude vibration problem of construction elements made of nanocomposites using shear deformation theory", *Materials*, **14**(14), 3843. https://doi.org/10.3390/ma14143843.

Fenjan, R.M., Faleh, N.M. and Ahmed, R.A. (2020), "Geometrical imperfection and thermal effects on nonlinear stability of microbeams made of graphene-reinforced nano-composites", *Adv. Nano Res.*, **9**(3), 147-156. https://doi.org/10.12989/anr.2020.9.3.147.

Fleck, N.A., Muller, G.M., Ashby, M.F. and Hutchinson, J.W. (1994), "Strain gradient plasticity: Theory and experiment", *Acta Metallurgica et Materialia*, **42**(2), 475-487. https://doi.org/10.1016/0956-7151(94)90502-9.

Ghannadpour, S.A.M., Karimi, M. and Tornabene, F. (2019), "Application of plate decomposition technique in nonlinear and post-buckling analysis of functionally graded plates containing crack", *Compos. Struct.*, **220**, 158-167. https://doi.org/10.1016/j.compstruct.2019.03.025.

Ghannadpour, S.A.M. and Moradi, F. (2019), "Nonlocal nonlinear analysis of nano-graphene sheets under compression using semi-Galerkin technique", *Adv. Nano Res.*, **7**(5), 311-324. http://doi.org/10.12989/anr.2019.7.5.311.

Ghannadpour, S.A.M., Moradi, F. and Tornabene, F. (2020), "Exact analytical solutions to the problem of relative post-buckling stiffness of thin nonlocal graphene sheets", *Thin Wall. Struct.*, **151**, 106712. https://doi.org/10.1016/j.tws.2020.106712.

Ghannadpour, S.A.M., Ovesy, H.R. and Nassirnia, M. (2012), "Buckling analysis of functionally graded plates under thermal loadings using the finite strip method", *Comput. Struct.*, **108**, 93-99. https://doi.org/10.1016/j.compstruc.2012.02.011.

Ghannadpour, S.A.M. and Shakeri, M. (2018), "Energy based collocation method to predict progressive damage behavior of imperfect composite plates under compression", *Latin Am. J. Solid Struct.*, **15**(4). https://doi.org/10.1590/1679-78254257.

Hadjesfandiari, A.R. and Dargush, G.F. (2016), "Couple stress theories: Theoretical underpinnings and practical aspects from a new energy perspective", *arXiv*, **1611**, 10249.

Hassanpour, P.A., Cleghorn, W.L., Esmailzadeh, E. and Mills, J.K. (2007), "Vibration analysis of micro-machined beam-type resonators", *J. Sound Vib.*, **308**(1-2), 287-301. https://doi.org/10.1016/j.jsv.2007.07.043.

Jena, S.K., Chakraverty, S. and Tornabene, F. (2019), "Dynamical behavior of nanobeam embedded in constant, linear, parabolic, and sinusoidal types of Winkler elastic foundation using first-order nonlocal strain gradient model", *Mater. Res. Exp.*, **6**(8), 0850f2. https://doi.org/10.1088/2053-1591/ab2779.

Jomehzadeh, E., Noori, H.R. and Saidi, A.R. (2011), "The size-dependent vibration analysis of micro-plates based on a modified couple stress theory", *Physica E*, **43**(4), 877-883. https://doi.org/10.1016/j.physe.2010.11.005.

Ke, L.L., Yang, J., Kitipornchai, S. and Bradford, M.A. (2012), "Bending, buckling and vibration of size-dependent functionally graded annular microplates", *Compos. Struct.*, **94**(11), 3250-3257. https://doi.org/10.1016/j.compstruct.2012.04.037.

Ke, L.L., Yang, J., Kitipornchai, S. and Wang, Y.S. (2014), "Axisymmetric postbuckling analysis of size-dependent functionally graded annular microplates using the physical neutral plane", *Int. J. Eng. Sci.*, **81**, 66-81. https://doi.org/10.1016/j.ijengsci.2014.04.005.

Koiter, W.T. (1969), "Couple-stresses in the theory of elasticity, I & II", *Philos. Transact. Royal Soc. London B*, **67**, 17-44.

Koizumi, M.F.G.M. (1997), "FGM activities in Japan", *Compos. Part B Eng.*, **28**(1-2), 1-4. https://doi.org/10.1016/S1359-8368(96)00016-9.

Lam, D.C., Yang, F., Chong, A.C.M., Wang, J. and Tong, P. (2003), "Experiments and theory in strain gradient elasticity", *J. Mech. Phys. Solids*, **51**(8), 1477-1508. https://doi.org/10.1016/S0022-5096(03)00053-X.

Lazopoulos, K.A. (2009), "On bending of strain gradient elastic micro-plates", *Mech. Res. Commun.*, **36**(7), 777-783. https://doi.org/10.1016/j.mechrescom.2009.05.005.

Mahmure, A., Sofiyev, A.H., Fantuzzi, N. and Kuruoglu, N. (2021), "Primary resonance of double-curved nanocomposite shells using nonlinear theory and multi-scales method: Modeling and analytical solution", *Int. J. Nonlinear Mech.*, **137**, 103816. https://doi.org/10.1016/j.ijnonlinmec.2021.103816.

Mehar, K., Mahapatra, T.R., Panda, S.K., Katariya, P.V. and Tompe, U.K. (2018), "Finite-element solution to nonlocal elasticity and scale effect on frequency behavior of shear deformable nano plate structure", *J. Eng. Mech.*, **144**(9), 04018094. https://doi.org/10.1061/(ASCE)EM.1943-7889.0001519.

Mindlin, R.D. (1965), "Second gradient of strain and surface-tension in linear elasticity", *Int. J. Solids Struct.*, **1**(4), 417-438.

https://doi.org/10.1016/0020-7683(65)90006-5.
Mindlin, R.D. and Tiersten, H.F. (1962), "Effects of couple-stresses in linear elasticity", *Arch. Ration. Mech. Anal.*, **11**(1), 415-448. https://doi.org/10.1007/BF00253946.
Mohammadi, M., Saidi, A.R. and Jomehzadeh, E. (2010), "Levy solution for buckling analysis of functionally graded rectangular plates", *Appl. Compos. Mater.*, **17**(2), 81-93. https://doi.org/10.1007/s10443-009-9100-z.
Monaco, G.T., Fantuzzi, N., Fabbrocino, F. and Luciano, R. (2021a), "Hygro-thermal vibrations and buckling of laminated nanoplates via nonlocal strain gradient theory", *Compos. Struct.*, **262**, 113337. https://doi.org/10.1016/j.compstruct.2020.113337
Monaco, G.T., Fantuzzi, N., Fabbrocino, F. and Luciano, R. (2021b), "Trigonometric solution for the bending analysis of magneto-electro-elastic strain gradient nonlocal nanoplates in hygro-thermal environment", *Mathematics*, **9**(5), 1-22. https://doi.org/10.3390/math9050567
Monaco, G.T., Fantuzzi, N., Fabbrocino, F. and Luciano, R. (2021c), "Critical temperatures for vibrations and buckling of magneto-electro-elastic nonlocal strain gradient plates", *Nanomaterials*, **11**(1), 87. https://doi.org/10.3390/nano11010087
Movassagh, A.A. and Mahmoodi, M.J. (2013), "A micro-scale modeling of Kirchhoff plate based on modified strain-gradient elasticity theory", *Eur. J. Mech. A Solids*, **40**, 50-59. https://doi.org/10.1016/j.euromechsol.2012.12.008.
Nix, W.D. (1989), "Mechanical properties of thin films", *Metall. Transact. A*, **20**(11), 2217. https://doi.org/10.1007/BF02666659.
Ovesy, H.R., Ghannadpour, S.A.M. and Nassirnia, M. (2015), "Post-buckling analysis of rectangular plates comprising functionally graded strips in thermal environments", *Comput. Struct*, **147**, 209-215. https://doi.org/10.1016/j.compstruc.2014.09.011.
Papargyri-Beskou, S. and Beskos, D.E. (2008), "Static, stability and dynamic analysis of gradient elastic flexural Kirchhoff plates", *Arch. Appl. Mech.*, **78**(8), 625-635. https://doi.org/10.1007/s00419-007-0166-5.
Papargyri-Beskou, S., Giannakopoulos, A.E. and Beskos, D.E. (2010), "Variational analysis of gradient elastic flexural plates under static loading", *Int. J. Solids Struct.*, **47**(20), 2755-2766. https://doi.org/10.1016/j.ijsolstr.2010.06.003.
Shariati, A., Barati, M.R., Ebrahimi, F. and Toghroli, A. (2020), "Investigation of microstructure and surface effects on vibrational characteristics of nanobeams based on nonlocal couple stress theory", *Adv. Nano Res.*, **8**(3), 191-202. https://doi.org/10.12989/anr.2020.8.3.191.
Sheng, H., Li, H., Lu, P. and Xu, H. (2010), "Free vibration analysis for micro-structures used in MEMS considering surface effects", *J. Sound Vib.*, **329**(2), 236-246. https://doi.org/10.1016/j.jsv.2009.08.035.
Taghizadeh, M., Ovesy, H. R. and Ghannadpour, S.A.M. (2015), "Nonlocal integral elasticity analysis of beam bending by using finite element method", *Struct. Eng. Mech.*, **54**(4), 755-769. https://doi.org/10.12989/sem.2015.54.4.755.
Tavakolian, F., Farrokhabadi, A. and Mirzaei, M. (2017), "Pull-in instability of double clamped microbeams under dispersion forces in the presence of thermal and residual stress effects using nonlocal elasticity theory", *Microsyst. Technol.*, **23**(4), 839-848. https://doi.org/10.1007/s00542-015-2785-z.
Thai, H.T. and Choi, D.H. (2013), "Size-dependent functionally graded Kirchhoff and Mindlin plate models based on a modified couple stress theory", *Compos. Struct.*, **95**, 142-153. https://doi.org/10.1016/j.compstruct.2012.08.023.
Toupin, R. (1962), "Elastic materials with couple-stresses", *Arch. Ration. Mech. Anal.*, **11**(1), 385-414. https://doi.org/10.1007/BF00253945.
Tsiatas, G.C. (2009), "A new Kirchhoff plate model based on a modified couple stress theory", *Int. J. Solid Struct.*, **46**(13), 2757-2764. https://doi.org/10.1016/j.ijsolstr.2009.03.004.
Tuna, M. and Trovalusci, P. (2020), "Scale dependent continuum approaches for discontinuous assemblies: 'Explicit' and 'implicit' non-local models", *Mech. Res. Commun.*, **103**, 103461. https://doi.org/10.1016/j.mechrescom.2019.103461
Wang, B., Zhao, J. and Zhou, S. (2010), "A micro scale Timoshenko beam model based on strain gradient elasticity theory", *Eur. J. Mech. A Solids*, **29**(4), 591-599. https://doi.org/10.1016/j.euromechsol.2009.12.005.
Yang, F.A.C.M., Chong, A.C.M., Lam, D.C.C. and Tong, P. (2002), "Couple stress based strain gradient theory for elasticity", *Int. J. Solids Struct.*, **39**(10), 2731-2743. https://doi.org/10.1016/S0020-7683(02)00152-X.
Zibaei, I., Rahnama, H., Taheri-Behrooz, F. and Shokrieh, M. M. (2014), "First strain gradient elasticity solution for nanotube-reinforced matrix problem", *Compos. Struct.*, **112**, 273-282. https://doi.org/10.1016/j.compstruct.2014.02.023

CC